Pooled CRISPR screening in pancreatic cancer cells implicates co-repressor complexes as a cause of multiple drug resistance via regulation of epithelial-to-mesenchymal transition

Author list:

Ryne C. Ramaker*[1,2]

Andrew A. Hardigan*[1,2]

Emily R. Gordon*[2]

Carter A. Wright[2,3]

Richard M. Myers[2]

Sara J. Cooper[2]

* These authors have contributed equally to this work

Corresponding author: Sara J. Cooper, sjcooper@hudsonalpha.org

Affiliations: [1]University of Alabama-Birmingham, Birmingham, AL 35294; [2]HudsonAlpha Institute for Biotechnology Huntsville, AL 35806; [3]University of Alabama Huntsville Huntsville, AL 35899

ABSTRACT

Pancreatic ductal adenocarcinoma (PDAC) patients suffer poor outcomes in part due to therapeutic resistance. We conducted four genome-wide CRISPR activation ($CRISPR_{act}$) and CRISPR knock out ($CRISPR_{ko}$) screens to identify novel resistance mechanisms to four cytotoxic chemotherapies (gemcitabine, 5-fluorouracil, irinotecan, and oxaliplatin). ABCG2, a well-described efflux pump was the strongest mediator of resistance. We showed that overexpressing HDAC1 altered promoter occupancy and expression of genes involved in the epithelial-to-mesenchymal transition. Using the results of our CRISPR screens, we predicted drug sensitivity for patients and cell lines based on gene expression profiles. These predictions could be clinically useful for treatment selection.

KEYWORDS

Genome-wide screen; CRISPR; pancreatic cancer; drug resistance; ABCG2; HDAC1; precision oncology

MAIN TEXT

Despite decades of work, pancreatic ductal adenocarcinoma (PDAC) has remained largely refractory to improvement of five-year survival rates, which are still less than 10% (1). Multi-drug combinations, such as FOLFIRINOX (fluorouracil, folinic acid, irinotecan and oxaliplatin), achieve, at best, modest improvements in patient outcomes (2). Unfortunately, many people with pancreatic cancer develop complete resistance to potent multi-drug cocktails (3). Cellular mechanisms of resistance have been explored by previous insertional mutagenesis- and RNA interference-based screens and have successfully identified genes whose inactivation leads to gemcitabine sensitivity in PDAC cells (4–6). Genome-wide CRISPR-Cas9 screening can provide complementary information (7, 8) and has identified essential genes in cell lines with *RNF43*-mutations (a recurrently mutated gene in PDAC) (9). These studies highlight the various mechanisms of cellular resistance and hint at the roles that genetic background and heterogeneity within tumors play in drug resistance (10).

The growing field of precision oncology aims to predict an optimal treatment for a patient based on tumor profiling. However, in the context of highly heterogeneous tumors, detection of genetic signatures associated with treatment response is difficult (11). One approach to this problem is to define the landscape of cellular mechanisms of PDAC drug resistance experimentally, then deeply screen tumors using a targeted approach for the presence of previously-identified resistance drivers. To achieve this goal, we performed CRISPR-Cas9 knock-out ($CRISPR_{ko}$) (12) and endogenous activation ($CRISPR_{act}$) (13) screening of 23,728 genes and 138,188 sgRNAs in two PDAC cell lines (BxPC3 and Panc-1) to identify genes whose loss or gain of expression were able to modulate sensitivity to four of the most common cytotoxic chemotherapies used in the treatment of PDAC (gemcitabine, oxaliplatin, irinotecan,

and 5-fluorouracil, **Figure 1A**, **S1A-B**).

We found the sgRNAs most strongly associated with drug resistance were highly drug-specific (Figure S1B) and replicates were significantly more correlated than samples treated with a different drug **(Figure S1C-F**). However, there was a much higher correlation between samples treated with different drugs than expected by chance, suggesting that mechanisms of resistance were sometimes shared between drugs in our study (**Figure S1C-F**). To prioritize resistance genes, we computed the sum of the replicate-minimum, $\log_2$ count fold change of the two most enriched sgRNAs targeting each gene (L2FC sum) in each cell line. We identified multi-drug resistance genes by computing the mean L2FC sum across all four drugs in each cell line (**Supplemental Table 1A-B**). This approach was particularly powerful because it leveraged information from 48 perturbations (4 drug screens x 3 replicates x 2 cell lines x 2 sgRNAs).

$CRISPR_{act}$ of the ATP-binding cassette (ABC) transporter, ABCG2, was the only perturbation that persistently induced resistance across each of the drug treatments in both of our cell lines **(Figure 1B-C**). Individual follow up of our top ABCG2 sgRNA showed that it induced a highly specific, 30-fold overexpression of ABCG2 (**Figure S2A**) and produced a resistance phenotype that was reversed with previously developed inhibitors of ABCG2 (**Figure S2B-C**). ABCG2 functions as an efflux pump with a broad range of substrates and has been associated with multi-drug resistance in several previous studies (14–16); this provides a strong validation of the efficacy of our multi-drug screening approach. Despite being the strongest signal associated with multi-drug resistance in our screen, ABCG2 does not appear to have significant relevance in PDAC patient tumors, as it is expressed at relatively low levels in all prognosis groups (**Figure S2D**). However, further analysis suggests that our screen has identified additional patient-relevant resistance genes (**Figure 1B**). We computed drug sensitivity scores

based on weighted expression level of resistance genes identified by our screen. Our algorithm PancDS is publicly available (https://github.com/rramaker/PancDS) and shows that those predictions readily segregate cell lines and patients into different treatment response groups (**Figure 1D**, **S3A-B**).

To identify other plausible mechanisms of multi-drug resistance with clinical relevance, we assessed whether there was enrichment of gene pathways associated with drug resistance or sensitivity based on our $CRISPR_{act}$ and $CRISPR_{ko}$ screens. Activation of chromatin remodeling genes was one of the most consistent mechanisms of drug resistance (**Figure 2A**, **Table S2**). Widespread chromatin repression has been previously associated with poor prognosis in PDAC patients (17). We performed targeted experiments with HDAC1, a gene that is known to cooperate with trans-acting repressors as a member of several transcriptional repressor complexes. Our top HDAC1 sgRNA induced greater than 10-fold overexpression of HDAC1. As one might expect, over-expression of this transcriptional regulator also produced several weaker transcriptional changes that we hypothesize to be downstream of HDAC1-mediated transcriptional regulation (**Figure 2B**). These downstream gene expression changes were particularly enriched for genes implicated in the epithelial-to-mesenchymal transition (EMT), a pathway known to mediate multi-drug resistance (**Figure 2B-C**) (18). Given HDAC1's function as a member of canonical repressor complexes, we were surprised to find that its activation also resulted in several up-regulated genes, including IMP2, TIMP1, ANXA1, and WNK1, which are involved in promoting a mesenchymal or stem cell state (19–22). $CRISPR_{act}$ of 11 other transcriptional repressors that were associated with resistance in our genome-wide screen (ARID4A, SMARCA4, SIN3A, SIN3B, SAP30, SAP18, RBBP7, MTA2, GATA2, CHD4, and BRMS1) also showed concordant up-regulation of at least one, but often several, of the same top

genes over-expressed upon HDAC1-activation (**Figure 2D**). ChIP-sequencing (ChIP-seq) of cells with activated HDAC1 uncovered a 3-fold increase the number of occupied sites relative to control cells and identified 17,501 occupied sites specific to HDAC1 activation (**Figure 2E**). These HDAC1-specific ChIP-seq peaks were highly enriched near the transcription start sites of genes differentially expressed upon HDAC1 activation (**Figure 2F**, **Figure S4**), suggesting a role for direct binding of HDAC1 in modulating their expression. Supporting this observed HDAC1 gene regulatory network, we found HDAC1-activated cells exhibited more cell migration in scratch assays relative to control cells (**Figure 2G-H**).

These data demonstrate the value of pooled CRISPR screening as a method for discovering cellular mechanisms of drug resistance. $\text{CRISPR}_{\text{act}}$ of *ABCG2* was the highest-confidence perturbation capable of inducing multi-drug resistance, but its clinical relevance is unclear. Some reports indicate that *ABCG2* is expressed uniquely in cancer stem cells, a minority of the total cell population; thus, *ABCG2'*s role may be obscured in bulk tumor sequencing (16). Leveraging our screen data to predict drug sensitivity in cell lines and patients based on their respective gene expression profiles demonstrate the potential application of these data, en masse, to direct personalized therapeutic approaches.

Our pathway-based analysis linked $\text{CRISPR}_{\text{act}}$ of several transcriptional repressor complex members to chemoresistance. Several chromatin remodeling genes, including *HDAC1*, induced a program of gene expression associated with EMT. The EMT pathway has been previously associated with chemoresistance in mouse models of PDAC where key EMT transcription factors were ablated (23). Chromatin remodeling genes have been linked to clinically relevant phenotypes in PDAC (24) including induction of EMT and increasing stem cell populations (25, 26). Our data provide evidence for *HDAC1* occupying the promoter regions

and regulating expression of several genes over-expressed upon $CRISPR_{act}$. Despite its canonical role as a repressor, HDAC complexes have recently been found to play a variety of roles in gene regulation (27). HDAC inhibitors have exhibited inconsistent results in clinical trials to date, an observation that has been partially attributed to a poor understanding of which HDAC classes are the best targets and which biomarkers indicate sensitivity to HDAC inhibition (28).

These data further our understanding of HDAC1 specifically and chromatin remodeling more generally in drug resistance and importantly the results of our large-scale screen provide additional avenues for exploration in the quest to improve treatment options for pancreatic cancer patients.

METHODS

Panc-1 (CRL-1469), BxPC3 (CRL-1687), and MiaPaca-2 (CRL-1420) cell lines were obtained from ATCC and cultured according to ATCC specifications. LentiCas9-Blast (Addgene #52962) or Lenti-dCAS9-VPS46-Blast (Addgene #61425) with lenti-MS2-p65-HSF1-Hygro (Addgene #61426) were used to generated cells stably expressing the knockout or gene activation machinery, respectively. The GeCKO A pooled sgRNA library (Addgene #1000000049) was used for gene knock out screening and the SAM pooled sgRNA library (Addgene #1000000057) was used for gene activation screening. LentiSAMv2 (Addgene #75112) was used for single gene activation. sgRNA library cloning, viral packaging and transduction method was previously described (25). Primer sequences are available in Table S3.

Library-transduced cells were under selection for one week post-transduction and expanded to $7x10^7$ cells per treatment replicate or 1000x representation for each of the 4 drug (gemcitabine, oxaliplatin, irinotecan and 5-fluorouracil) and control conditions per replicate. A

minimum 500x representation was maintained at all times in control cells. Drug treatment doses were optimized to yield ~80% cell death relative to untreated control cells after 14 days of culture. After 14 days of drug treatment, cells were pelleted and stored at -80°C. DNA extraction and library preparation was performed as previously described (29). Three sets of replicates (control and 4 drug treated samples) for each cell line were sequenced on one lane of Illumina NextSeq resulting in an average of 40 million reads per sample. We ranked each of the sgRNAs targeting each gene by the minimum $\log_2$ fold change across each replicate.

To identify top genes from our genome-wide screen, we prioritized genes by the "L2FC sum" in each cell line, which is the sum of the replicate minimum $\log_2$ fold changes of the top two sgRNAs targeting each gene. Multi-drug hits were prioritized by computing the mean "L2FC sum" of the four drug treatments.

Pathway enrichment significance was determined using a Wilcox-ranked sum test based on Reactome Pathways (**Table S2**) (30). Cell lines over-expressing chromatin remodelers, including HDAC1 were characterized using RNA-sequencing and ChIP-sequencing data generation and analysis using well established, published methods (31, 32) (https://www.encodeproject.org/documents/).

Cell migration was measured using scratch assays on MiaPaCa-2 cells. Time to close half the gap was calculated for each well (33).

Additional methodological details are available in the Supplemental Information.

DATA AVAILABILITY

ABCG2 RNA-sequencing data are available at GEO using the accessions GSE131596.

RNA-sequencing and ChIP-sequencing data for chromatin remodelers are available using the GEO accession GSE158541.

Raw sequencing data from the screen are available through SRA using the project ID PRJNA542321.

AUTHOR CONTRIBUTIONS

RCR, AAH, ERG, CAW and SJC designed the experiments. RCR, AAH, CAW, and ERG collected data. RCR, AAH, SJC, and ERG analyzed the data. RCR, AAH, and SJC wrote the first draft. All authors contributed to writing of the paper and read and approved the final manuscript.

CONFLICT OF INTEREST DISCLOSURES

None reported.

ACKNOWLEDGEMENTS

We thank the Myers and Cooper labs for helpful feedback. We also thank HudsonAlpha Discovery's Genome Services Lab for assistance and optimizing the sequencing parameters of our CRIPSR screen. We also acknowledge The Cancer Genome Atlas, Cancer Cell Line Encyclopedia Project datasets, which were extremely valuable and without which this study would not be possible. This work was supported by the State Cancer Fund of Alabama (to RMM). RCR and AAH were funded by the UAB MSTP (NIH-NIGMS 5T32GM008361-21. SJC and ERG were supported by the HudsonAlpha Tie the Ribbons Fund. SJC received support from

the UAB CCTS grant (NIH 1UL1TR001417-01) and the UAB Comprehensive Cancer Center (NIH 5P30CA013148).

REFERENCES

1. R. L. Siegel, K. D. Miller, A. Jemal, Cancer statistics, 2018. *CA. Cancer J. Clin.* **68**, 7–30 (2018).
2. T. Conroy, *et al.*, FOLFIRINOX versus Gemcitabine for Metastatic Pancreatic Cancer. *N. Engl. J. Med.* **364**, 1817–1825 (2011).
3. I. Garrido-Laguna, M. Hidalgo, Pancreatic cancer: from state-of-the-art treatments to promising novel therapies. *Nat. Rev. Clin. Oncol.* **12**, 319–334 (2015).
4. V. Bhattacharjee, Y. Zhou, T. Yen, A synthetic lethal screen identifies the Vitamin D receptor as a novel gemcitabine sensitizer in pancreatic cancer cells. *Cell Cycle* **13**, 3839–3856 (2014).
5. L. You, D. Chang, H.-Z. Du, Y.-P. Zhao, Genome-wide screen identifies PVT1 as a regulator of Gemcitabine sensitivity in human pancreatic cancer cells. *Biochem. Biophys. Res. Commun.* **407**, 1–6 (2011).
6. S. C. Smith, *et al.*, A gemcitabine sensitivity screen identifies a role for NEK9 in the replication stress response. *Nucleic Acids Res.* **42**, 11517–27 (2014).
7. B. Evers, *et al.*, CRISPR knockout screening outperforms shRNA and CRISPRi in identifying essential genes. *Nat. Biotechnol.* **34**, 631–3 (2016).
8. D. W. Morgens, R. M. Deans, A. Li, M. C. Bassik, Systematic comparison of CRISPR/Cas9 and RNAi screens for essential genes. *Nat. Biotechnol.* **34**, 634–6 (2016).

9. Z. Steinhart, *et al.*, Genome-wide CRISPR screens reveal a Wnt–FZD5 signaling circuit as a druggable vulnerability of RNF43-mutant pancreatic tumors. *Nat. Med.* **23**, 60–68 (2017).

10. S. Yachida, C. A. Iacobuzio-Donahue, The Pathology and Genetics of Metastatic Pancreatic Cancer. *Arch Pathol Lab Med—Vol* **133** (2009).

11. M. Griffith, *et al.*, Optimizing Cancer Genome Sequencing and Analysis. *Cell Syst.* **1**, 210–223 (2015).

12. T. Wang, J. J. Wei, D. M. Sabatini, E. S. Lander, Genetic Screens in Human Cells Using the CRISPR-Cas9 System. *Science (80-.).* **343**, 80–84 (2014).

13. S. Konermann, *et al.*, Genome-scale transcriptional activation by an engineered CRISPR-Cas9 complex. *Nature* **517**, 583–8 (2015).

14. W. Mo, J.-T. Zhang, Human ABCG2: structure, function, and its role in multidrug resistance. *Int. J. Biochem. Mol. Biol.* **3**, 1–27 (2012).

15. Y. Sun, *et al.*, Gemcitabine upregulates ABCG2/BCRP and modulates the intracellular pharmacokinetic profiles of bioluminescence in pancreatic cancer cells. *Anticancer. Drugs* **27**, 183–191 (2016).

16. V. J. Bhagwandin, J. M. Bishop, W. E. Wright, J. W. Shay, The Metastatic Potential and Chemoresistance of Human Pancreatic Cancer Stem Cells. *PLoS One* **11**, e0148807 (2016).

17. O. G. McDonald, *et al.*, Epigenomic reprogramming during pancreatic cancer progression links anabolic glucose metabolism to distant metastasis. *Nat. Genet.* **49**, 367–376 (2017).

18. K. A. Song, A. C. Faber, Epithelial-to-mesenchymal transition and drug resistance: Transitioning away from death. *J. Thorac. Dis.* **11**, E82–E85 (2019).

19. C. Dahlem, A. Barghash, P. Puchas, J. Haybaeck, S. M. Kessler, The insulin-like growth factor 2 mRNA binding protein IMP2/IGF2BP2 is overexpressed and correlates with poor survival in pancreatic cancer. *Int. J. Mol. Sci.* **20**, 1–8 (2019).

20. R. C. D'Angelo, *et al.*, TIMP-1 via TWIST1 induces EMT phenotypes in human breast epithelial cells. *Mol. Cancer Res.* **12**, 1324–1333 (2014).

21. S. Maschler, *et al.*, Annexin A1 attenuates EMT and metastatic potential in breast cancer. *EMBO Mol. Med.* **2**, 401–414 (2010).

22. H. A. Dbouk, *et al.*, Actions of the protein kinase WNK1 on endothelial cells are differentially mediated by its substrate kinases OSR1 and SPAK. *Proc. Natl. Acad. Sci. U. S. A.* **111**, 15999–16004 (2014).

23. X. Zheng, *et al.*, EMT Program is Dispensable for Metastasis but Induces Chemoresistance in Pancreatic Cancer. *Nature* **527**, 525–530 (2015).

24. G. Lomberk, *et al.*, Distinct epigenetic landscapes underlie the pathobiology of pancreatic cancer subtypes. *Nat. Commun.* **9**, 1–10 (2018).

25. M. H. Cai, *et al.*, Depletion of HDAC1, 7 and 8 by Histone Deacetylase Inhibition Confers Elimination of Pancreatic Cancer Stem Cells in Combination with Gemcitabine. *Sci. Rep.* **8**, 1–11 (2018).

26. A. Nihan Kilinc, *et al.*, Histone deacetylases, Mbd3/NuRD, and Tet2 hydroxylase are crucial regulators of epithelial–mesenchymal plasticity and tumor metastasis. *Oncogene* **39**, 1498–1513 (2020).

27. G. E. Adams, A. Chandru, S. M. Cowley, Co-repressor, co-activator and general transcription factor: The many faces of the Sin3 histone deacetylase (HDAC) complex. *Biochem. J.* **475**, 3921–3932 (2018).

28. E. Hessmann, S. A. Johnsen, J. T. Siveke, V. Ellenrieder, Epigenetic treatment of pancreatic cancer: Is there a therapeutic perspective on the horizon? *Gut* **66**, 168–179 (2017).

29. J. Joung, *et al.*, Genome-scale CRISPR-Cas9 knockout and transcriptional activation screening. *Nat. Protoc.* **12**, 828–863 (2017).

30. A. Fabregat, *et al.*, The Reactome Pathway Knowledgebase. *Nucleic Acids Res.* **46**, D649–D655 (2018).

31. S. G. Landt, *et al.*, ChIP-seq guidelines and practices of the ENCODE and modENCODE consortia. *Genome Res.* **22**, 1813–1831 (2012).

32. N. H. Boyd, *et al.*, Chromodomain Helicase DNA-Binding Protein 7 Is Suppressed in the Perinecrotic/Ischemic Microenvironment and Is a Novel Regulator of Glioblastoma Angiogenesis. *Stem Cells* **37**, 453–462 (2019).

33. A. Grada, M. Otero-Vinas, F. Prieto-Castrillo, Z. Obagi, V. Falanga, Research Techniques Made Simple: Analysis of Collective Cell Migration Using the Wound Healing Assay. *J. Invest. Dermatol.* **137**, e11–e16 (2017).

FIGURE LEGENDS

Figure 1. CRISPR screen reveals drug resistance genes. (A) Schematic describing our screening protocol. (B) A scatterplot shows the mean L2FC sum for all four drugs assayed in each of two cell lines compared to the log10 p-value for the association of the same gene's expression with with patient survival. ABCG2 stands out as the most highest L2FC over all four drugs (C) Boxplots indicate the sgRNA fold change in counts per million comparing treated cells to control cells for each replicate and each cell line for the top *ABCG2* sgRNA. Circles represent data from Panc-1 cells. Squares represent BXPC-3 (D) Using weighted averages derived from the screen data we predicted likely sensitivity to gemcitabine based on expression of resistance-associated genes (PKG). There is a significant difference in survival between patients with predicted high versus low gemcitabine sensitivity (p=0.01, Chi-squared test).

Figure 2. A) Scatter plot showing pathways enriched for multi-drug resistance in our $CRISPR_{act}$ and $CRISPR_{ko}$ screens and their association with patient survival in the TCGA cohort. Patient survival is represented by the size and color of the circle. B) A volcano plot shows that activation of HDAC1 expression using a dCas9-activation approach results in strong over-expression of HDAC1 based on RNA-sequencing. (C) Pathway enrichment analysis shows that HDAC1 overexpression especially affects epithelial to mesenchymal transition (EMT), cell efflux, apoptosis, autophagy, and DNA repair. P-values reported are derived from Fisher's exact test comparing observed versus expected number of genes in each pathway. Full pathway list available in Table S2. (D) Overexpression of each of the target genes listed on top right quadrant leads to a similar pattern of over-expression of genes shown on the lower right. (E) ChIP-seq

analysis reveals ChIP-seq peaks in the control (CTL) MiaPaCa-2 cells overlap significantly with MiaPaCa-2 cells over-expressing HDAC1 (red). An additional 17501 peaks are identified with over-expression of HDAC1. (F) Cumulative distribution plot showing that HDAC1 binding sites identified upon over-expression of HDAC1 (blue) are nearby transcription start sites (TSS) of differentially expressed genes. (G) Scratch assay shows that over-expression of HDAC1 leads to increased migration compared to control cells (H) Quantification of the scratch assays shows a significant difference with HDAC1 overexpression (Student's T-test).

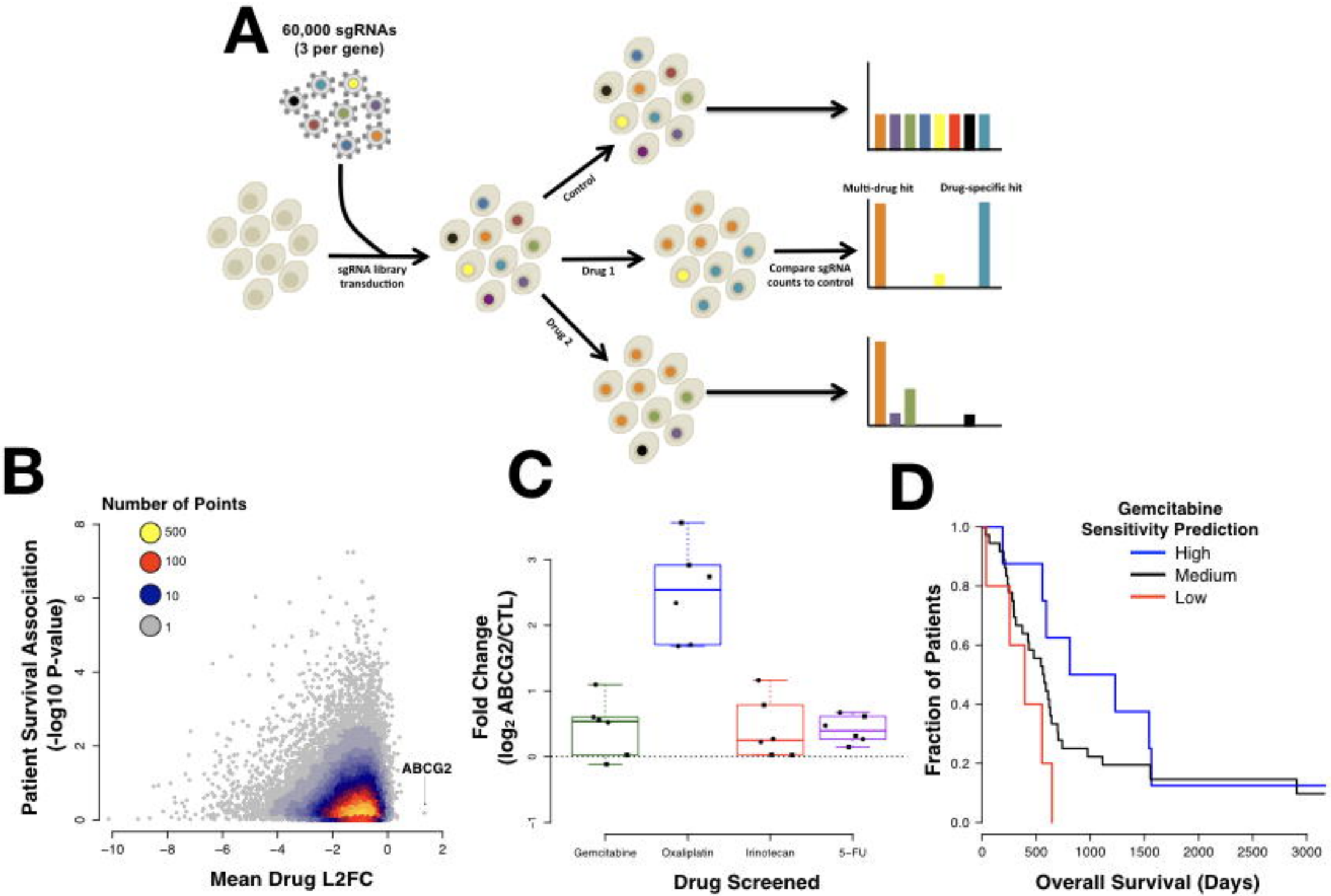
A
60,000 sgRNAs
(3 per gene)
sgRNA library
transduction
Control
Drug 1
Drug 2
Compare sgRNA
counts to control
Multi-drug hit
Drug-specific hit
B
Number of Points
500
100
10
1
Patient Survival Association
(-log10 P-value)
ABCG2
Mean Drug L2FC
C
Fold Change
(log2 ABCG2/CTL)
Gemcitabine
Oxaliplatin
Irinotecan
5-FU
Drug Screened
D
Gemcitabine
Sensitivity Prediction
High
Medium
Low
Fraction of Patients
Overall Survival (Days)

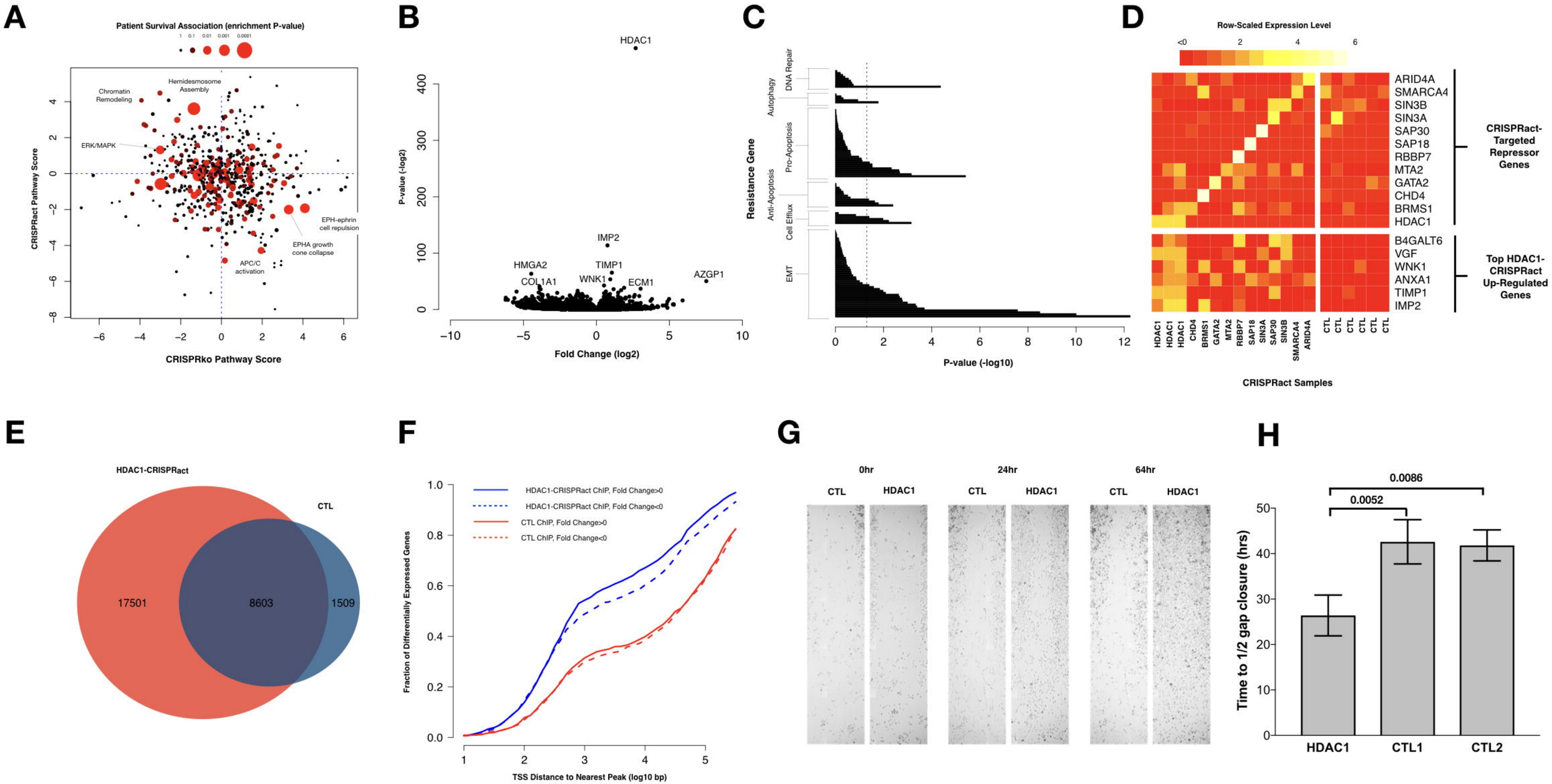
A
Patient Survival Association (enrichment P-value)
1 0.1 0.01 0.001 0.0001
Chromatin Remodeling
Hemidesmosome Assembly
ERK/MAPK
EPH-ephrin cell repulsion
EPHA growth cone collapse
APC/C activation
CRISPRact Pathway Score
CRISPRko Pathway Score
B
HDAC1
IMP2
HMGA2
COL1A1
TIMP1
WNK1
ECM1
AZGP1
P-value (-log2)
Fold Change (log2)
C
Resistance Gene
DNA Repair
Autophagy
Pro-Apoptosis
Anti-Apoptosis
Cell Efflux
EMT
P-value (-log10)
D
Row-Scaled Expression Level
<0 2 4 6
ARID4A
SMARCA4
SIN3B
SIN3A
SAP30
SAP18
RBBP7
MTA2
GATA2
CHD4
BRMS1
HDAC1
CRISPRact-Targeted Repressor Genes
B4GALT6
VGF
WNK1
ANXA1
TIMP1
IMP2
Top HDAC1-CRISPRact Up-Regulated Genes
HDAC1 HDAC1 HDAC1 CHD4 BRMS1 GATA2 MTA2 RBBP7 SAP18 SIN3A SAP30 SIN3B SMARCA4 ARID4A
CTL CTL CTL CTL CTL CTL
CRISPRact Samples
E
HDAC1-CRISPRact
CTL
17501
8603
1509
F
HDAC1-CRISPRact ChIP, Fold Change>0
HDAC1-CRISPRact ChIP, Fold Change<0
CTL ChIP, Fold Change>0
CTL ChIP, Fold Change<0
Fraction of Differentially Expressed Genes
TSS Distance to Nearest Peak (log10 bp)
G
0hr
24hr
64hr
CTL
HDAC1
H
0.0086
0.0052
Time to 1/2 gap closure (hrs)
HDAC1
CTL1
CTL2